Tris(butadiene) Metal Complexes of the First Row Transition Metals Versus Coupling of Butadiene to Eight and Twelve-Carbon Hydrocarbon Chains

Qunchao Fan,[a*] Huidong Li,[a] Jia Fu,[a] Zhixiang Fan,[a] Yonggen Xu, [a] Hao Feng,[a] Yaoming Xie,[b] R. Bruce King,[b*] and Henry F. Schaefer III[b]

[a]*School of Science, Key Laboratory of High Performance Scientific Computation, Xihua University, Chengdu, China 610039*

[b]*Department of Chemistry and Center for Computational Quantum Chemistry University of Georgia, Athens, Georgia 30602, USA*

rbking@chem.uga.edu; fanqunchao@mail.xhu.edu.cn

Abstract

The role that zerovalent nickel plays in catalyzing the trimerization of butadiene to 1,5,9-cyclododecatriene conveys interest in the properties of the tris(butadiene)metal complexes $(C_4H_6)_3M$. In this connection the complexes $(C_4H_6)_3M$ (M = Ti to Ni) of the first row transition metals have been investigated by density functional theory. The intermediate $C_{12}H_{18}Ni$ which has been isolated in the nickel-catalyzed trimerization of butadiene but too unstable for X-ray crystallography, is suggested here to have an open chain hexahapto $\eta^{3,3}$-$C_{12}H_{18}$ ligand rather than the octahapto such ligand suggested by some investigators. The lowest energy $(C_4H_6)_3M$ structures of the other first row transition metals from vanadium to cobalt are found to have related structures with open chain $C_{12}H_{18}$ ligands having hapticities ranging from four to eight with hexahapto structures being most common. The nickel and cobalt $(C_{12}H_{18})M$ derivatives favor low-spin singlet and doublet spin states, respectively, whereas the manganese derivative $(C_{12}H_{18})Mn$ favors the high-spin sextet state corresponding to the half-filled d^5 shell of Mn(II). A $(C_4H_6)_3Cr$ structure with three separate tetrahapto butadiene ligands analogous to the very stable $(\eta^4\text{-}C_4H_6)_3M$ (M = Mo, W) with the favored 18-electron metal configuration is found to be a very high energy structure relative to isomers containing an open chain $C_{12}H_{18}$ ligand.

1. Introduction

The chemistry of butadiene transition metal complexes predates the groundbreaking 1951 discovery of ferrocene[1,2] by approximately two decades. Thus Reihlen and coworkers in 1930[3] first synthesized butadiene-iron tricarbonyl as an essentially air-stable volatile yellow liquid using the simple thermal reaction of butadiene with iron pentacarbonyl in a sealed vessel. A reinvestigation of this product by Hallam and Pauson in 1958[4] after the discovery of ferrocene suggested a $(\eta^4\text{-}C_4H_6)Fe(CO)_3$ structure with coordination of both butadiene double bonds to the iron atom thereby giving the iron atom the favored 18-electron configuration (Figure 1). This structure was subsequently confirmed by Mills and Robinson[5] using X-ray crystallography.

$(\eta^4\text{-}C_4H_6)Fe(CO)_3$ $(\eta^4\text{-}C_4H_6)_3M$ (M = Mo, W)

Figure 1. Examples of experimentally known butadiene metal complexes.

The synthesis of stable homoleptic butadiene metal complexes is more challenging because of the tendency of butadiene to dimerize or trimerize on a transition metal site. However, the zerovalent cobalt 1,4-bis(trimethylsilyl)butadiene derivative $[(Me_3Si)_2C_4H_4]_2Co$ was synthesized and structurally characterized in 1996.[6] In this system the bulky trimethylsilyl substituents inhibit butadiene dimerization or trimerization. Our recent theoretical studies on the unsubstituted bis(butadiene) compounds of the first row transition metals, $(C_4H_6)_2M$. show that the preferred spin states of the $(C_4H_6)_2M$ complexes can be rationalized on the basis of strong tetrahedral ligand field metal complexes.[7] As for tris(butadiene)metal complexes, the very stable species $(C_4H_6)_3M$ with the favored 18-electron metal configuration are known for the second and third row transition metals molybdenum and tungsten but not for the first row transition metal chromium (Figure 1). These $(C_4H_6)_3M$ (M = Mo, W) complexes can be synthesized by cocondensation of metal vapors with butadiene[8] or by reduction of metal halides with activated magnesium in the presence of butadiene.[9] X-ray crystallography indicates trigonal prismatic coordination of the six C=C double bonds of the three butadiene ligands to the central metal atom.

The reaction of zerovalent nickel systems with butadiene is of particular interest, since it provides an efficient catalytic route to 1,5,9-cyclododecatriene from butadiene, thereby making this 12-membered ring hydrocarbon readily available.[10,11,12,13,14] An intermediate bis(butadiene)nickel, $(C_4H_6)_2Ni$ would have the favored 18-electron configuration and may be present in the yellow liquid obtained by cocondensation of nickel vapor with butadiene at –78°C. [15] A related unstable bis(2,3-dimethylbutadiene)nickel, $(2,3\text{-}MeC_4H_4)_2Ni$ has been synthesized at low temperatures as red-brown crystals which decompose above –10°C. [16] These bis(butadiene)nickel derivatives readily take up additional butadiene to form a volatile red $C_{12}H_{18}Ni$ compound.[17] Hydrogenation of this species gives *n*-dodecane indicating that the $C_{12}H_{18}$ ligand has an open chain of 12 carbon atoms. Influenced by the 18-electron rule, this $C_{12}H_{18}Ni$ was originally formulated as the bis(allylic) olefin complex $(\eta^{3,2,3}\text{-}C_{12}H_{18})Ni$ with the central nickel atom bonded to two trihapto allylic units and one C=C double bond of the $C_{12}H_{18}$ chain (Figure 2). This formulation was also consistent with the crystallographically determined structures of its protonation products $[(\eta^{3,2,2}\text{-}C_{12}H_{19})Ni]^+X^-$ (X = PF_6^-. SO_3F) indicating an acyclic $C_{12}H_{19}$ ligand bonded to the nickel atom through two C=C double bonds and a terminal allylic unit.[18] The C_{12} unit in the acyclic neutral $C_{12}H_{18}Ni$ complex readily cyclizes to form $(\eta^{2,2,2}$-1,5,9-cyclododecatriene)nickel of which the structurally characterized [19] *trans*,*trans*,*trans* stereoisomer is greatly favored over the other possible stereoisomers. The free 1,5,9-cyclododecatriene is readily displaced from its complex with excess butadiene, thereby completing the cycle for the nickel-catalyzed trimerization of butadiene to 1,5,9-cyclododecatriene. Mechanistic aspects of this nickel-catalyzed trimerization of butadiene have been considered by Tobisch using density functional theory.[20]

The ability of zerovalent nickel systems to catalyze the trimerization of butadiene to 1,5,9-cyclododecatriene can be related to bis(butadiene)nickel already having the favored 18-electron configuration. Thus in order for a central nickel atom to accommodate more than two butadiene ligands without exceeding the 18-electron configuration, some of the C=C double bonds in the set of butadiene ligands cannot complex to the nickel atom. This makes them reactive towards C–C bond formation in oligomerization reactions, thereby converting sp^2 carbon atoms of the original butadiene molecules into sp^3 carbon atoms.

Early transition metals differ from nickel by being able to complex with three butadiene ligands without exceeding the favored 18-electron configuration. In the second and third row transition metal series, this is indicated by the isolation of the very stable tris(butadiene) derivatives of molybdenum and tungsten, $(\eta^4\text{-}C_4H_6)_3M$ (M = Mo, W)

(Figure 1).[8,9] However, the corresponding chromium compound $(\eta^4\text{-}C_4H_6)_3Cr$ has never been reported. In order the explore the possible existence of stable tris(butadiene) derivatives of the first row transition metals, we have used density functional theory to explore the $(C_4H_6)_3M$ systems for all of the first row transition metals from titanium and nickel. Our results, reported here, predict dimerization or trimerization of butadiene at all first row transition metal sites, even chromium, rather than the formation of $(C_4H_6)_3M$ complexes with three separate butadiene ligands.

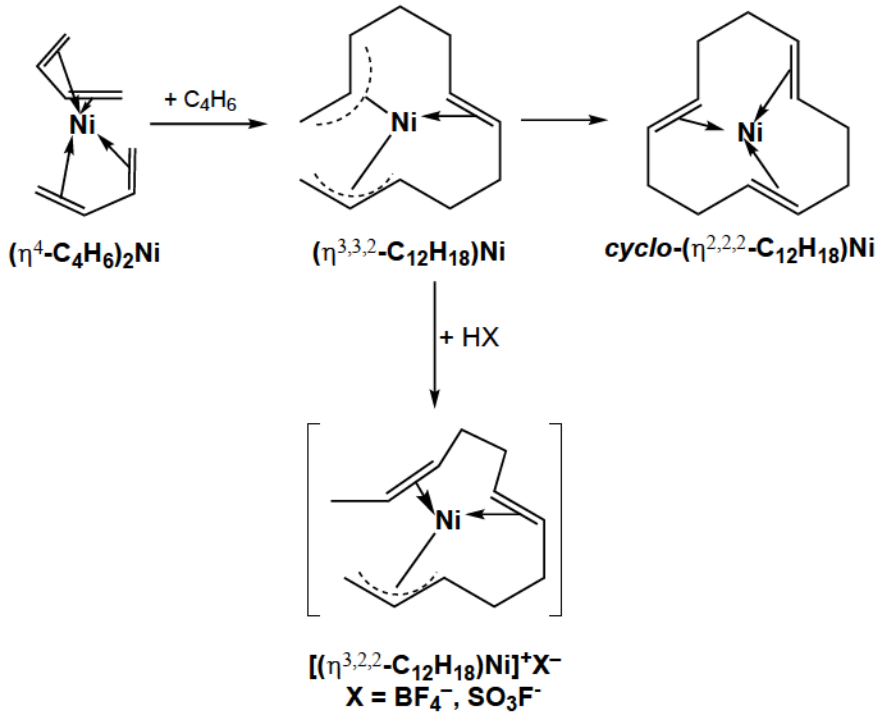

Figure 2. Complexes from the interaction of zerovalent nickel with butadiene.

2. Theoretical Methods

Electron correlation effects are included to some degree by using density functional theory (DFT) methods, which have evolved as a practical and effective computational tool, especially for organometallic compounds.[21,22,23,24,25,26,27] Initially two very differently constructed DFT methods, namely the B3LYP and the BP86 methods, were used in the present study. The B3LYP method is a hybrid HF/DFT method, combining the three-parameter Becke functional with the Lee-Yang-Parr generalized gradient correlation functional.[28,29] The BP86 method combines Becke's 1988 exchange functional with Perdew's 1986 gradient-corrected correlation functional.[30,31] However, Reiher and coworkers have found that B3LYP favors the high-spin state while BP86 favors the low-spin state.[32] This is also true for the

molecules studied in the present research, so that these two DFT methods sometimes predict global minima of different spin states. For this reason, Reiher and coworkers proposed a new parametrization for the B3LYP functional, named B3LYP*, which provides many electronic state orderings in agreement with experiment.[33] In the present paper, we use the B3LYP* method as the third method, in order to predict more reliable spin splittings. Only the B3LYP* results are discussed in the present manuscript; the results from the B3LYP and BP86 methods are listed in the Supporting Information. We also used a hybrid meta-GGA DFT method, M06-L,[34] which was developed by Truhlar's group and suggested for the study of organometallic and inorganic thermochemistry. Our M06-L geometries and energetics are comparable to other results and are also listed in the Supporting Information.

Double-ζ plus polarization (DZP) basis sets were used. For carbon atoms one set of spherical harmonic d functions (with the exponent $\alpha_d(C) = 0.75$) was added to the standard Huzinaga-Dunning contracted DZ sets. This basis set is designated (9s5p1d/4s2p1d).[35,36] For hydrogen atoms, a set of p polarization functions $\alpha_p(H) = 0.75$ was added to the Huzinaga-Dunning DZ sets. For the first row transition metals, in our loosely contracted DZP basis sets, the Wachters primitive sets were used, but augmented by two sets of p functions and one set of d functions, contracted following Hood et al., and designated (14s11p6d/10s8p3d).[37,38]

The geometries of all structures were fully optimized using the four DFT methods. The harmonic vibrational frequencies and the corresponding infrared intensities were determined analytically at the same levels. All of the computations were carried out with the Gaussian 09 program,[39] in which the fine grid, i.e., the pruned (75, 302) grid, is the default for evaluating integrals numerically.

The $(C_4H_6)_3M$ structures (M = Ti, Cr, Fe, Ni) were optimized in the singlet, triplet, and quintet electronic states, whereas the odd-electron $(C_4H_6)_3M$ structures (M = V, Mn, Co) were optimized in the doublet, quartet, and sextet electronic states. The optimized geometries of the energetically low-lying (within 30 kcal/mol) species of $(C_4H_6)_3M$ are shown in Figures 3 to 9. Each structure is designated as **M-nX**, where **M** is the symbol of the central metal atom, **n** orders the structure according their relative energies predicted by the B3LYP* method, and **X** designates the spin states, using **S**, **D**, **T**, **Q**, **P** and **H** for the singlets, doublets, triplets, quartets, quintets, and sextets, respectively.

The molecules $[Ni(C_{12}H_{19})]^+X^-$ (X = BF_4, F_3CSO_3) are experimentally known.[18] Initially we studied the $[Ni(C_{12}H_{19})]^+$ cation using the DZP B3LYP* method. The optimized geometry of the cation is reported in Table S109 (in Supporting Information). Our theoretical Ni-C and C-C bond distances are in good agreement with the

experimental results within 0.05 Å. This indicates that our method is suitable for the present study.

3. Results

3.1 Molecular Structures

3.1.1. $(C_4H_6)_3Ni$. In 1972, Skell and coworkers reported the reaction of nickel atoms with butadiene to produce dodeca-2,6,10-triene-1,12-diylnickel.[15] The authors suggested an octahapto $\eta^{3,2,3}$-$C_{12}H_{18}$ ligand in order to give the nickel atom the favored 18-electron configuration. However, in the present study, all attempts to find such a structure with an octahapto $\eta^{3,2,3}$-$C_{12}H_{18}$ ligand failed. Instead, our geometry optimizations always led to structures containing a hexahapto $\eta^{3,3}$-$C_{12}H_{18}$ ligand with an uncomplexed central C=C double bond thereby giving the nickel atom a 16-electron rather than an 18-electron configuration.

The four $Ni(C_4H_6)_3$ structures within 22 kcal/mol of the lowest energy structure **Ni-1S** are all singlets with hexahapto straight chain $C_{12}H_{18}$ ligands of various types but all with one uncomplexed C=C double bond (Figure 3 and Table 1). In the lowest energy such structure **Ni-1S** the three carbons at each end of the C_{12} chain are bonded to the central nickel atom as trihapto allylic ligands leaving an uncomplexed C=C double bond of length 1.347 Å (B3LYP*) in the center of the chain. Structures **Ni-2S** and **Ni-3S,** lying 6.7 and 8.9 kcal/mol, respectively, in energy above **Ni-1S**, have similar geometries with a hexahapto $\eta^{3,2,1}$-$C_{12}H_{18}$ ligand. In the latter a terminal allylic unit, the central C=C double bond, and an interior carbon atom from the other terminal allylic unit are all within bonding distance of the nickel atom. The difference between **Ni-2S** and **Ni-3S** is the orientation of their terminal uncomplexed C=C double bonds. The hexahapto $\eta^{3,2,1}$-$C_{12}H_{18}$ ligand in **Ni-4S**, lying 9.5 kcal/mol in energy above **Ni-1S**, has a terminal allylic unit at one end of the C_{12} chain and the carbon atom at the other end of the C_{12} chain in addition to the central C=C double bond. These four singlet $(C_4H_6)_3Ni$ structures **Ni-1S** through **Ni-4S** have a low-spin configuration for the nickel atom with a 16-electron configuration.

The relatively high energy singlet structure **Ni-5S** at 27.6 kcal/mol (B3LYP*, Table 1) above **Ni-1S** has one tetrahapto butadiene ligand and one chelating C_8H_{12} ligand forming a nine-membered C_8Ni ring containing two uncoordinated C=C double bonds of lengths 1.36 Å (B3LYP*) (Figure 3 and Table 1). In **Ni-5S**, as in the four lower energy singlet $(C_4H_6)_3Ni$ structures, the central nickel atom has a low-spin singlet 16-electron configuration.

Table 1. Relative energies (ΔE in kcal/mol), relative energies with zero-point energy correction (ΔE_{ZPE} in kcal/mol), relative enthalpies (ΔH in kcal/mol), and spin expectation values $\langle S^2 \rangle$ for the $(C_4H_6)_3Ni$ structures. None of the optimized structures reported in this paper has any imaginary vibrational frequencies.

	Ni-1S (C_1)	Ni-2S (C_1)	Ni-3S (C_1)	Ni-4S (C_1)	Ni-5S (C_1)	Ni-1T (C_1)	Ni-2T (C_1)
ΔE	0.0	6.7	8.9	9.5	27.6	22.5	28.6
ΔE_{ZPE}	0.0	6.5	9.0	9.6	20.2	20.4	26.9
ΔH(298K)	0.0	6.6	8.9	9.6	22.4	21.1	27.4
$\langle S^2 \rangle$	0.00	0.00	0.00	0.00	0.00	2.03	2.02

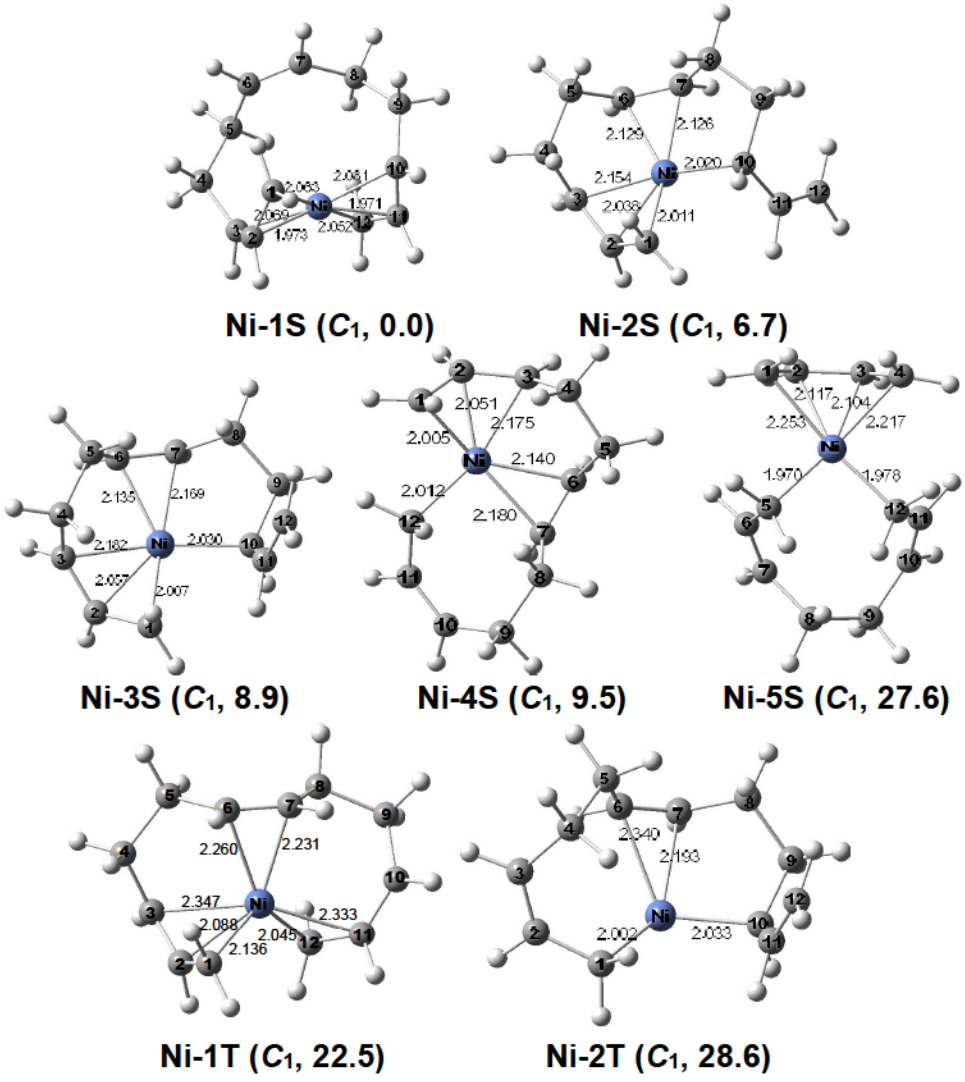

Figure 3. The low-energy optimized $(C_4H_6)_3Ni$ structures obtained by the B3LYP* method. In Figures 3 to 9 the distances (in Å) were.

The triplet structures **Ni-1T** and **Ni-2T** have higher energies, lying 22.5 and 28.6 kcal/mol (B3LYP*), respectively above **Ni-1S** (Figure 3 and Table 1). Structure **Ni-1T** has a heptahapto $\eta^{3,2,2}$-$C_{12}H_{18}$ ligand, while structure **Ni-2T** has a tetrahapto $\eta^{1,2,1}$-$C_{12}H_{18}$ ligand bonded to the nickel atom through the central C=C double bond and the terminal carbon atoms. Thus, the Ni atom in **Ni-1T** has a 17-electron configuration, while that in **Ni-2T** has a 14-electron configuration. The effect of spin contamination with the B3LYP method was reported to be negligible.[40] It is also true in our study of **Ni-1T** and **Ni-2T**, for which their spin expectation values $\langle S^2 \rangle$ are 2.03 and 2.02, respectively. These are very close to the ideal $\langle S^2 \rangle$ value of 2.00 for triplet spin state structures..

3.1.2. $(C_4H_6)_3Co$. Seven low-energy $(C_4H_6)_3Co$ structures were found (Figure 4 and Table 2). The lowest energy structure is the doublet **Co-1D** having a hexahapto $\eta^{3,3}$-$C_{12}H_{18}$ ligand with an uncoordinated C=C double bond of length 1.348 Å (B3LYP*). The $\eta^{3,3}$-$C_{12}H_{18}$ ligand in **Co-1D** is similar to that in **Ni-1S**. The second doublet structure **Co-2D**, lying 8.5 kcal/mol (B3LYP*) in energy above **Co-1D,** also has all three butadiene units coupled into a $C_{12}H_{18}$ chain. However, the hexahapto bonding of the $\eta^{3,2,1}$-$C_{12}H_{18}$ ligand in **Co-2D** is different from that in **Co-1D** but similar to that in **Ni-3S,** involving only one terminal allylic unit as well as the central C=C double bond, and the interior carbon atom of the other allylic unit. This leaves an uncomplexed C=C double bond in **Co-2D** at the end of the C_{12} chain rather than in the center of the chain.

The three remaining doublet $(C_4H_6)_3Co$ structures are all high-energy structures (Figure 4 and Table 2). Structure **Co-3D**, lying 20.9 kcal/mol in energy above **Co-1D**, has three separate butadiene ligands. One of the butadiene ligands is a tetrahapto ligand and the two remaining butadiene ligands are dihapto ligands thereby giving the central cobalt atom a 17-electron configuration consistent with the doublet spin state. Structure **Co-4D**, lying 25.9 kcal/mol (B3LYP*) in energy above **Co-1D**, has a similar geometry to **Co-3D.** Structures **Co-3D** and **Co-4D** differ only in the relative orientations of the two dihapto butadiene ligands. The even higher energy structure **Co-5D**, lying 34.6 kcal/mol in energy above **Co-1D**, has one tetrahapto butadiene ligand and one chelating C_8H_{12} ligand forming a nine-membered C_8Co ring containing two uncoordinated C=C double bonds of lengths ~1.36 Å (B3LYP*). The bonding of the C_8H_{12} unit in **Co-5D** is thus similar to that in **Ni-5S**.

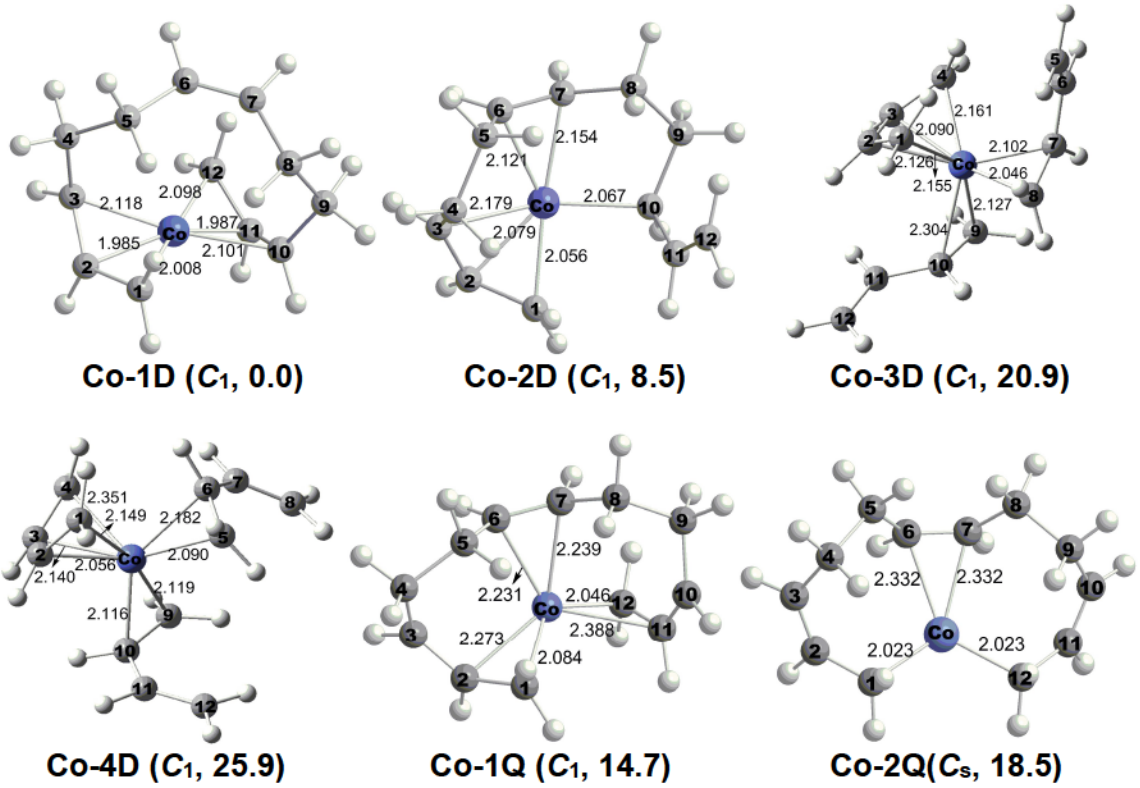

Figure 4. The low-energy optimized $(C_4H_6)_3Co$ structures obtained by the B3LYP* method.

Table 2. Relative energies (ΔE in kcal/mol), relative energies with zero-point energy correction (ΔE_{ZPE} in kcal/mol), relative enthalpies (ΔH in kcal/mol), and spin expectation values $\langle S^2 \rangle$ for the $(C_4H_6)_3Co$ structures.

	Co-1D (C_1)	**Co-2D** (C_1)	**Co-3D** (C_1)	**Co-4D** (C_1)	**Co-1Q** (C_1)	**Co-2Q** (C_s)
ΔE	0.0	8.5	20.9	25.9	14.7	18.5
ΔE_{ZPE}	0.0	8.4	16.2	21.1	13.1	16.7
ΔH(298K)	0.0	8.4	17.8	22.8	13.5	17.2
$\langle S^2 \rangle$	0.78	0.79	0.82	0.81	3.80	3.78

The lowest energy quartet $(C_4H_6)_3Co$ structure **Co-1Q**, lying 14.7 kcal/mol above **Co-1D** has a coupled $C_{12}H_{18}$ ligand in which three C=C double bonds are bonded to the central cobalt atom (Figure 4 and Table 2). The second quartet structure **Co-2Q**, lying 18.5 kcal/mol (B3LYP*) in energy above **Co-1D** has a tetrahapto $\eta^{1,2,1}$-$C_{12}H_{18}$ ligand similar to that in the triplet $(C_4H_6)_3Ni$ structure **Ni-2T**. In the quartet $(C_4H_6)_3Co$ structures the cobalt atom in **Co-1Q** has the expected 15-electron configuration for a quartet whereas the cobalt atom in **Co-2Q** has only a 13-electron configuration.

The unrestricted DFT (B3LYP*) method used in this paper predicts small spin contamination for the five doublet $(C_4H_6)_3Co$ structures with the spin expectation values $\langle S^2 \rangle$ ranging from 0.78 to 0.82, compared with the ideal $\langle S^2 \rangle$ value of 0.75 for doublet spin states. The $\langle S^2 \rangle$ values for the quartet structures are in the narrow range of 3.78 to 3.80, compared with the ideal $\langle S^2 \rangle$ value of 3.75 for quartet spin states.

3.1.3. $(C_4H_6)_3Fe$. Seven low-energy $(C_4H_6)_3Fe$ structures were found (Figure 5 and Table 3). The lowest energy $(C_4H_6)_3Fe$ structure by B3LYP* is a triplet structure **Fe-1T** with an octahapto $\eta^{3,2,3}$-$C_{12}H_{18}$ ligand, thereby providing the iron atom with a 16-electron configuration consistent with a triplet spin state. A second triplet $(C_4H_6)_3Fe$ structure **Fe-2T**, lying only 0.9 kcal/mol (B3LYP*) above **Fe-1T**, has a hexahapto $\eta^{3,3}$-$C_{12}H_{18}$ ligand similar to that in **Ni-2S** and **Co-1D,** with an uncomplexed central C=C double bond of length 1.347 Å (B3LYP). This gives the iron atom in **Fe-2T** only a 14-electron configuration. Since **Fe-1T** and **Fe-2T** are essentially isoenergetic, either one could be the global minimum. The much higher energy triplet $(C_4H_6)_3Fe$ structure **Fe-3T**, lying 22.7 kcal/mol above **Fe-1T**, has three separate butadiene ligands. One of these butadiene ligands is a tetrahapto ligand whereas the other two butadiene ligands are dihapto ligands. This gives the iron atom in **Fe-3T** a 16-electron configuration, consistent with its triplet spin state.

The lowest energy quintet $(C_4H_6)_3Fe$ structure **Fe-1P**, lying 8.1 kcal/mol in energy above **Fe-1T**, has a coupled $C_{12}H_{18}$ ligand in which three C=C double bonds are bonded to the central cobalt atom (Figure 5 and Table 3). This gives the iron atom in **Fe-1P** a 14-electron configuration consistent with its quintet spin state. This hexahapto bonding of the $C_{12}H_{18}$ ligand in the quintet $(C_4H_6)_3Fe$ structure **Fe-1P** (Figure 5) is similar to that in the quartet $(C_4H_6)_3Co$ structure **Co-1Q**. The other quintet $(C_4H_6)_3Fe$ structure**,** lying 16.8 kcal/mol (B3LYP*) in energy above **Fe-1T**, has a tetrahapto $C_{12}H_{18}$ ligand in which a C=C double bond at each end of the C_{12} chain is bonded to the central iron atom.

The lowest energy singlet $(C_4H_6)_3Fe$ structure **Fe-1S**, lying 9.8 kcal/mol in energy above **Fe-1T**, has a coupled $\eta^{3,2,3}$-$C_{12}H_{18}$ ligand with allylic units at each end and the central C=C double bond bonded to the iron atom leading to eight Fe–C bonds thereby giving the iron atom a 16-electron configuration (Figure 5 and Table 3). The other singlet $(C_4H_6)_3Fe$ structure **Fe-2S** is a much higher energy structure, lying 31.0 kcal/mol (B3LYP*) above **Fe-1T**. Structure **Fe-2S** has three separate butadiene ligands. Two of the butadiene ligands in **Fe-2S** are tetrahapto ligands, whereas the third butadiene ligand is only a dihapto ligand. This gives the central iron atom the favored 18-electron configuration.

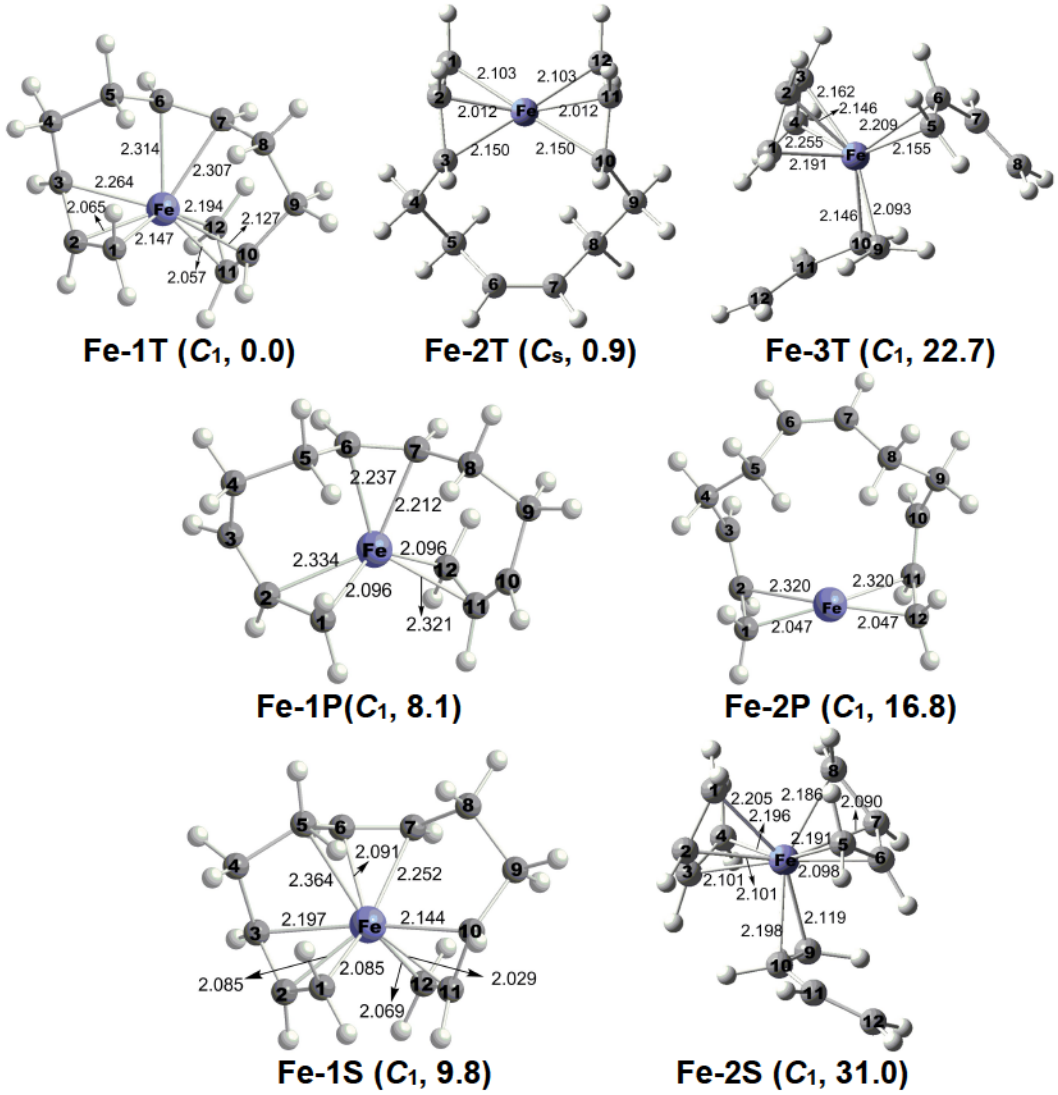

Figure 5. The low-energy optimized $(C_4H_6)_3Fe$ structures obtained by the B3LYP* method.

Table 3. Relative energies (ΔE in kcal/mol), relative energies with zero-point energy correction (ΔE_{ZPE} in kcal/mol), relative enthalpies (ΔH in kcal/mol), and the spin expectation values $\langle S^2 \rangle$ for the $(C_4H_6)_3Fe$ structures.

	Fe-1T (C_1)	Fe-2T (C_s)	Fe-3T (C_1)	Fe-1P (C_1)	Fe-2P (C_1)	Fe-1S (C_1)	Fe-2S (C_1)
ΔE	0.0	0.9	22.7	8.1	16.8	9.8	31.0
ΔE_{ZPE}	0.0	0.6	18.0	6.9	15.2	10.5	29.1
ΔH(298K)	0.0	0.7	19.8	7.3	16.0	10.0	29.6
$\langle S^2 \rangle$	2.12	2.09	2.25	6.08	6.05	0.00	0.00

3.1.4. $(C_4H_6)_3Mn$. High-spin electronic states are expected to be energetically favored for this manganese system. Seven low-energy structures were optimized for $(C_4H_6)_3Mn$, namely three doublets, two quartets, and two sextets (Figure 6 and Table 4). The global minimum predicted by the B3LYP* method is the high-spin sextet structure **Mn-1H** in which the three butadiene units have coupled to form a linear hexahapto $\eta^{2,2,2}$-$C_{12}H_{18}$ ligand with two uncomplexed C=C double bonds of length 1.316 Å (B3LYP*). This gives the manganese atom a 13-electron configuration consistent with the sextet spin state. In the other sextet $(C_4H_6)_3Mn$ structure **Mn-2H**, lying only 3.1 kcal/mol above **Mn-1H,** the three butadiene units are combined to form a $\eta^{1,2,1}$-$C_{12}H_{18}$ ligand. However, this ligand is only a tetrahapto ligand similar to the $\eta^{1,2,1}$-ligands in the **Co-2Q** and **Ni-2T** structures discussed above. The manganese atom in **Mn-2H** is highly unsaturated with an 11-electron configuration. Note that **Mn-2H** is only slightly higher in energy than **Mn-1H** so that either structure could be observed experimentally.

All of the lower spin $(C_4H_6)_3Mn$ structures, namely quartet and doublet structures, lie at least 20 kcal/mol above the two sextet structures **Mn-1H** and **Mn-2H**. This reflects the stability of d^5 Mn(II) in the sextet spin state with a half-filled d shell and implies that the $C_{12}H_{18}$ ligands in **Mn-1H** and **Mn-2H** are formally dianions. The quartet $(C_4H_6)_3Mn$ structure **Mn-1Q**, lying 20.5 kcal/mol (B3LYP*) in energy above **Mn-1H**, has three separate dihapto η^2-C_4H_6 ligands (Figure 6 and Table 4). The other quartet structure **Mn-2Q**, lying 25.0 kcal/mol (B3LYP*) in energy above **Mn-1H**, has a coupled tetrahapto $\eta^{3,1}$-C_8H_{12} ligand with an uncomplexed C=C double bond of length 1.357 Å (B3LYP*) and a dihapto butadiene ligand with an uncomplexed C=C double bond of length 1.352 Å (B3LYP*). In both quartet structures the manganese atom has a 13-electron configuration.

The doublet structures **Mn-1D** and **Mn-3D**, lying 23.9 and 27.5 kcal/mol (B3LYP*) in energy above **Mn-1H,** have two tetrahapto butadiene ligands and one dihapto butadiene ligand (Figure 6 and Table 4). This gives the manganese atoms in each structure a 17-electron configuration for the doublet spin state. Structures **Mn-1D** and **Mn-3D** differ in the orientations of their butadiene ligands. The other doublet structure **Mn-2D**, lying 25.9 kcal/mol (B3LYP*) in energy above **Mn-1H**, has the three butadiene units coupled to form an octahapto $\eta^{3,2,3}$-$C_{12}H_{18}$ ligand, thereby giving the manganese atom a 15-electron configuration.

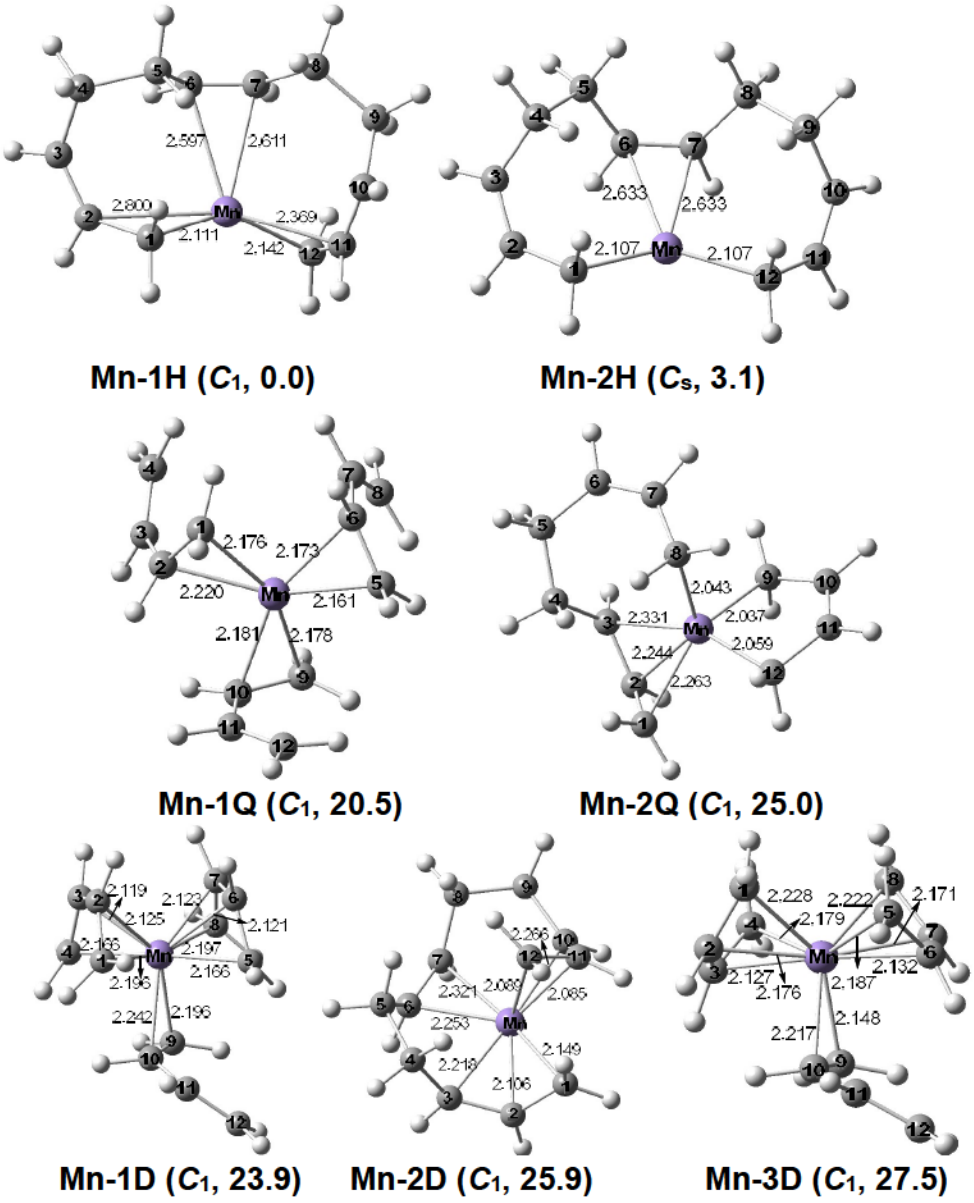

Figure 6. The low-energy optimized $(C_4H_6)_3Mn$ structures obtained by the B3LYP* method.

Table 4. Relative energies (ΔE in kcal/mol), relative energies with zero-point energy correction (ΔE_{ZPE} in kcal/mol), relative enthalpies (ΔH in kcal/mol), and spin expectation values $\langle S^2 \rangle$ for the $(C_4H_6)_3Mn$ structures.

	Mn-1H (C_1)	Mn-2H (C_s)	Mn-1Q (C_1)	Mn-2Q (C_1)	Mn-1D (C_1)	Mn-2D (C_1)	Mn-3D (C_1)
ΔE	0.0	3.1	20.5	25.0	23.9	25.9	27.5
ΔE_{ZPE}	0.0	2.9	16.3	21.9	22.2	28.3	26.4
ΔH(298K)	0.0	2.9	17.9	22.2	22.2	27.2	26.3
$\langle S^2 \rangle$	8.78	8.78	4.06	4.01	0.89	0.82	0.83

3.1.5. $(C_4H_6)_3Cr$. Seven low-energy $(C_4H_6)_3Cr$ structures were found, namely two singlets, three triplets, and two quintets (Figure 7 and Table 3). The B3LYP* method predicts the quintet structure **Cr-1P** to be the global minimum. In **Cr-1P**, the three C_4H_6 ligands are coupled to form a long chain $\eta^{3,3}$-$C_{12}H_{18}$ ligand with a central uncomplexed C=C double bond of length 1.356 Å (B3LYP*) thereby giving the chromium atom a 12-electron configuration consistent with a quintet spin state. The quintet structure **Cr-2P**, lying only 0.8 kcal/mol in energy above **Cr-1P**, has similar geometry to **Cr-1P**, with the three C_4H_6 ligands coupled to form a long chain $\eta^{3,3}$-$C_{12}H_{18}$ ligand with an uncomplexed central C=C double bond. Structures **Cr-1P** and **Cr-2P** differ only in the relative orientation of the trihapto bonding interactions at each end of the C_{12} chain. Note that **Cr-1P** and **Cr-2P** are essentially isoenergetic.

The triplet $(C_4H_6)_3Cr$ structure **Cr-1T**, lying only 2.3 kcal/mol in energy above **Cr-1P**, has a coupled straight chain $\eta^{3,3}$-C_8H_{12} ligand and a separate η^4-C_4H_6 ligand thereby giving the chromium atom a 16-electron configuration consistent with the triplet spin state (Figure 7 and Table 3). In the significantly higher energy triplet structure **Cr-2T**, lying 15.3 kcal/mol (B3LYP*) above **Cr-1P**, there is a long chain $\eta^{3,2,3}$-$C_{12}H_{18}$ ligand thereby giving the chromium atom a 14-electron configuration. The other triplet structure **Cr-3T**, lying 17.4 kcal/mol in energy above **Cr-1P**, has two tetrahapto η^4-C_4H_6 ligands and one dihapto η^2-C_4H_6 ligand. This gives the chromium atom in **Cr-3T** a 16-electron configuration.

Table 5. Relative energies (ΔE in kcal/mol), relative energies with zero-point energy correction (ΔE_{ZPE} in kcal/mol), relative enthalpies (ΔH in kcal/mol), and spin expectation values $\langle S^2 \rangle$ for the $(C_4H_6)_3Cr$ structure. Neither structure has any imaginary vibrational frequencies.

	Cr-1P (*C*1)	**Cr-2P** (*Cs*)	**Cr-1T** (*C*1)	**Cr-2T** (*C*1)	**Cr-3T** (*C*1)	**Cr-1S** (*C*1)	**Cr-2S** (*C*1)
ΔE	0.0	0.8	2.3	15.3	17.4	28.5	39.5
ΔE_{ZPE}	0.0	0.6	1.5	16.2	14.2	26.8	38.2
ΔH(298K)	0.0	0.7	1.3	15.5	14.9	26.9	38.2
$\langle S^2 \rangle$	6.07	6.07	2.18	2.13	2.14	0.00	0.00

The B3LYP* method predicts the two singlet structures **Cr-1S** and **Cr-2S** to have high energies of 28.5 and 39.5 kcal/mol**,** respectively, above **Cr-1P**. Structure **Cr-1S** has a geometry similar to **Cr-3T** thereby representing a low-spin complex with a 16-electron chromium configuration. The other singlet $(C_4H_6)_3Cr$ structure **Cr-2S** has

three tetrahapto butadiene ligands thereby giving the chromium atom the favored 18-electron configuration. This high-energy $(C_4H_6)_3Cr$ structure **Cr-2S** is analogous to the experimentally known $(C_4H_6)_3M$ (M = Mo, W) complexes of the heavier group 6 metals molybdenum and tungsten.[8,9]

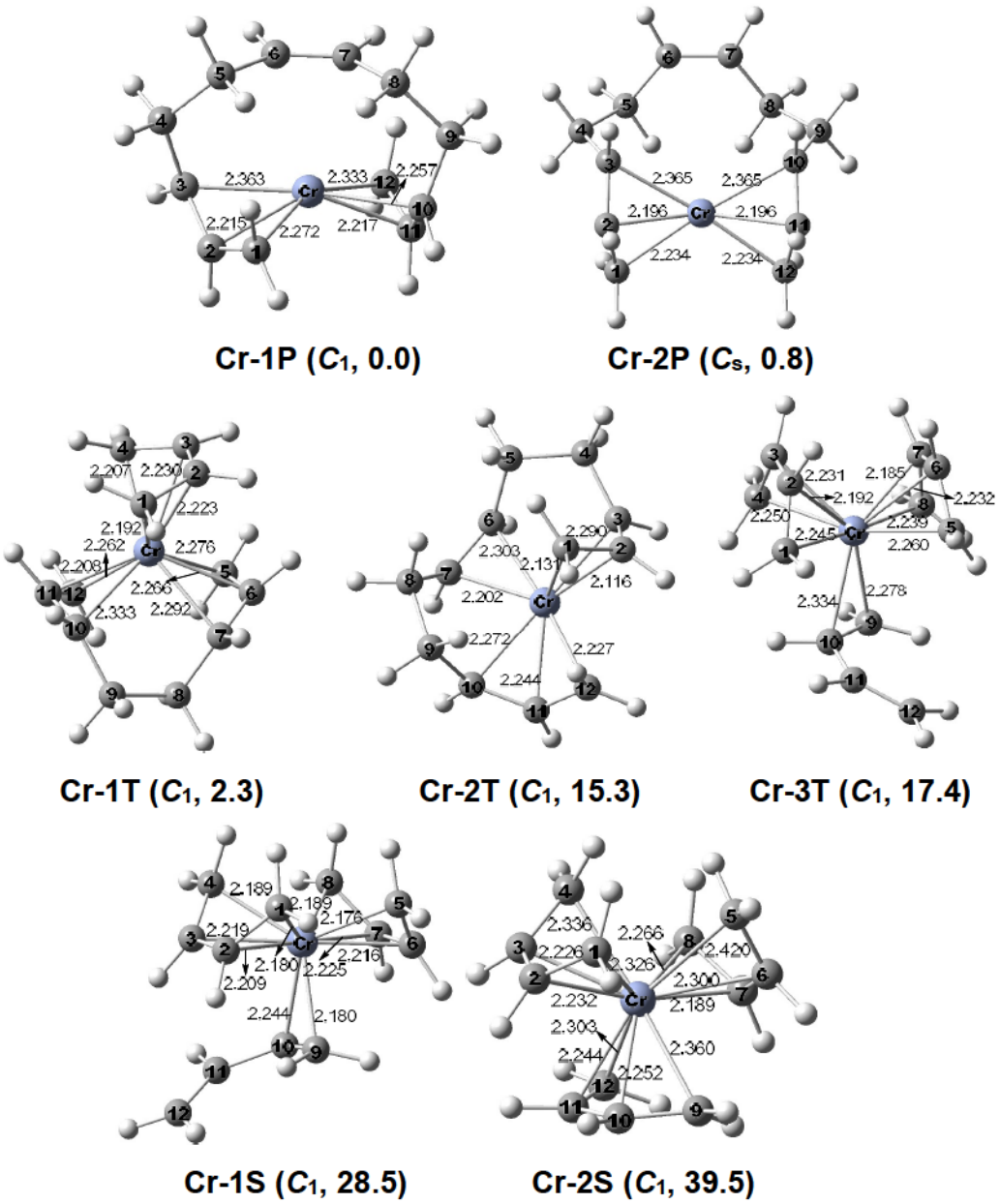

Figure 7. The low-energy optimized $(C_4H_6)_3Cr$ structures obtained by the B3LYP* method.

3.1.6. $(C_4H_6)_3V$. Nine low-energy $(C_4H_6)_3V$ structures were found, namely four doublet structures **V-1D, V-2D, V-3D**, and **V-4D**, and five quartet structures **V-1Q, V-2Q, V-3Q, V-4Q**, and **V-5Q** (Figure 2 and Table 2). The lowest energy $(C_4H_6)_3V$ structure is the quartet **V-1Q** predicted by B3LYP*, in which the three C_4H_6 ligands are coupled to form a long chain octahapto $\eta^{3,2,3}$-$C_{12}H_{18}$ ligand with two terminal trihapto allylic units and a central C=C double bond all bonded to the central vanadium atom. This gives the vanadium atom in **V-1Q** a 13-electron configuration consistent with a quartet spin state. Structure **V-2Q**, lying 10.5 kcal/mol in energy above **V-1Q**, has a similar long-chain $\eta^{3,2,3}$-$C_{12}H_{18}$ ligand as **V-1Q** but with a different ligand stereochemistry. The still higher energy $(C_4H_6)_3V$ structure **V-3Q**, lying 20.7 kcal/mol in energy above **V-1Q**, also has a straight chain $\eta^{3,2,1}$-$C_{12}H_{18}$ ligand, but with only six rather than eight carbons within bonding distance of the vanadium atom. Therefore in **V-3Q** the central vanadium atom has only a 11-electron configuration.

Higher energy quartet $(C_4H_6)_3V$ structures are found with three separate butadiene ligands. Thus **V-4Q** and **V-5Q** lie 21.2 and 21.6 kcal/mol (B3LYP*), respectively, in energy above **V-1Q** (Figure 2 and Table 2). In both **V-4Q** and **V-5Q** two of the three butadiene ligands are tetrahapto ligands whereas the third butadiene ligand is a dihapto ligand with an uncomplexed C=C double bond. This gives the vanadium atom in both **V-4Q** and **V-5Q** a central 15-electron configuration consistent with their quartet spin states.

The doublet $(C_4H_6)_3V$ structure **V-1D**, lying only 4.4 kcal/mol (B3LYP*) above the global minimum **V-1Q**, has a coupled long chain $\eta^{3,2,3}$-$C_{12}H_{18}$ ligand, thereby giving the vanadium atom a 13-electron configuration (Figure 2 and Table 2). The doublet structure **V-1D**, with a 13-electron vanadium configuration, is a low-spin configuration of the quartet $(C_4H_6)_3V$ structure **V-1Q**. Note that **V-1D** is only slightly (< 5 kcal/mol) higher in energy than **V-1Q**, so that either could be observed experimentally. The second doublet $(C_4H_6)_3V$ structure **V-2D**, lying 9.8 kcal/mol (B3LYP*) in energy above **V-1Q**, has three separate tetrahapto butadiene ligands in contrast to **V-1D** where all three C_4H_6 units are coupled into a single $C_{12}H_{18}$ ligand. The three separate tetrahapto butadiene ligands in **V-2D** give the vanadium a 17-electron configuration, as expected for a doublet spin state. The higher energy doublet $(C_4H_6)_3V$ structures **V-3D** and **V-4D**, lie 14.8 and 28.7 kcal/mol (B3LYP*), respectively, above **V-1Q**. These two structures have long chain $\eta^{3,2,1}$ $C_{12}H_{18}$ ligands with an uncomplexed C=C double bond leading to 11-electron configurations for the central vanadium atom. Structures **V-3D** and **V-4D** differ in the location of the uncomplexed C=C double bond. Thus, the uncomplexed C=C double bond is internal in **V-3D** but terminal in **V-4D**.

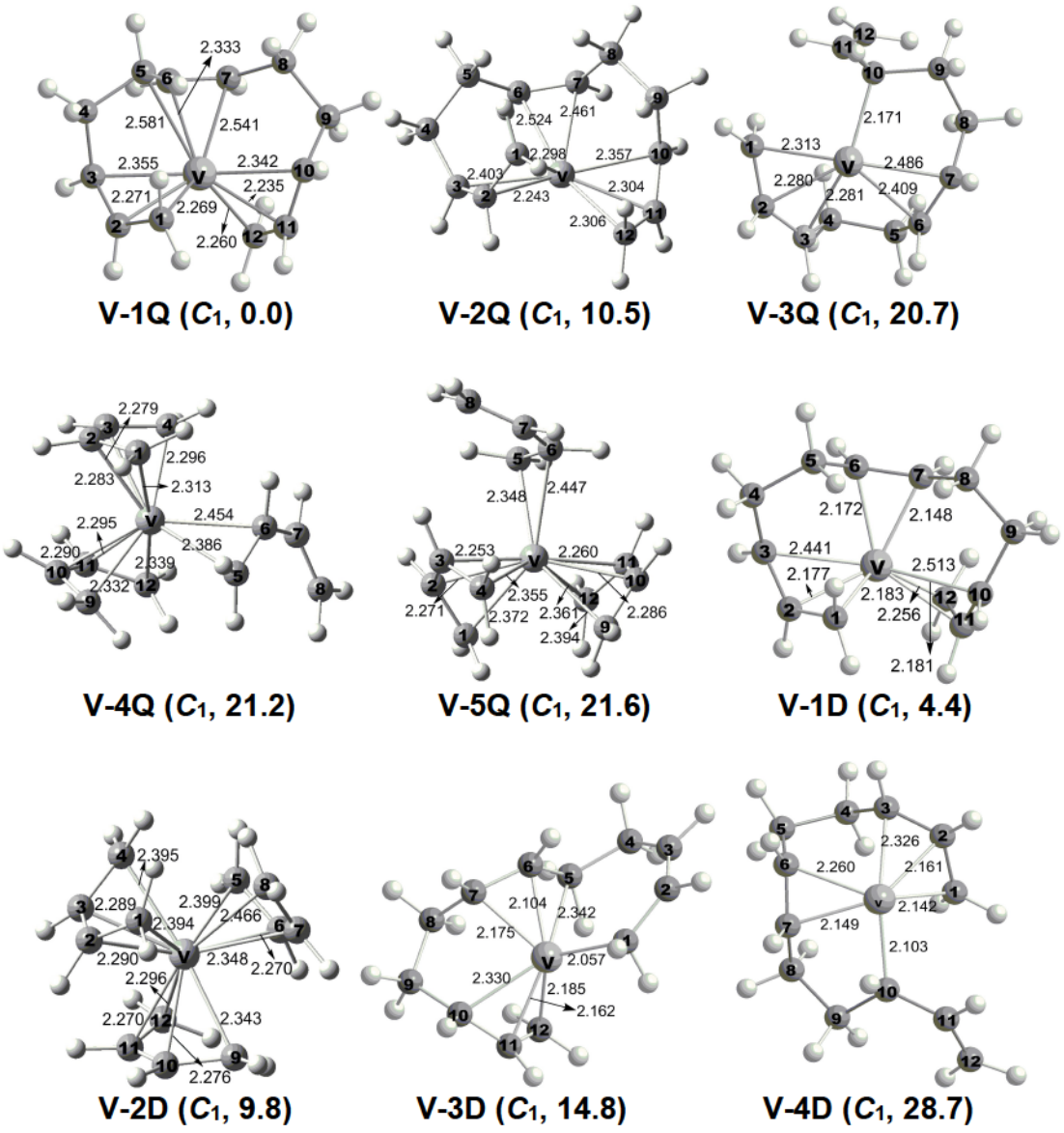

Figure 8. The low-energy optimized $(C_4H_6)_3V$ structures obtained by the B3LYP* method.

Table 6. Relative energies (ΔE in kcal/mol), relative energies with zero-point energy correction (ΔE_{ZPE} in kcal/mol), relative enthalpies (ΔH in kcal/mol), and spin expectation values $\langle S^2 \rangle$ for the $(C_4H_6)_3V$ structure. Neither structure has any imaginary vibrational frequencies.

	V-1Q (C_1)	V-2Q (C_1)	V-3Q (C_1)	V-4Q (C_1)	V-5Q (C_1)	V-1D (C_1)	V-2D (C_1)	V-3D (C_1)	V-4D (C_1)
ΔE	0.0	10.5	20.7	21.2	21.6	4.4	9.8	14.8	28.7
ΔE_{ZPE}	0.0	11.1	16.9	20.7	17.6	4.7	8.0	13.7	28.0
ΔH(298K)	0.0	11.2	18.3	20.9	19.0	4.5	8.4	13.6	28.1
$\langle S^2 \rangle$	3.78	3.79	3.79	3.78	3.79	0.77	0.79	0.77	0.79

3.1.7. $(C_4H_6)_3Ti$. Three low-energy $(C_4H_6)_3Ti$ structures were found, i.e., two singlets and one triplet (Figure 9 and Table 7). The global minimum by B3LYP* is the singlet structure **Ti-1S**. In **Ti-1S**, the Ti-C distances clearly indicate that one of the C_4H_6 ligands is tetrahapto, and the remaining two C_4H_6 ligands are coupled to form an acyclic $\eta^{3,3}$-C_8H_{12} ligand. Thus, the titanium atom has a 14-electron configuration. The other singlet structure **Ti-2S**, lying 15.5 kcal/mol (B3LYP*) in energy above **Ti-1S**, is shown by its Ti-C distances to have three separate tetrahapto η^4-C_4H_6 ligands, thereby giving the titanium atom a 16-electron configuration similar to that in the experimentally known $(\eta^5\text{-}C_5H_5)Ti(\eta^7\text{-}C_7H_7)$.[41] The triplet $(C_4H_6)_3Ti$ structure **Ti-1T** has a similar geometry to **Ti-1S**, but lies 22.8 kcal/mol (B3LYP*) in energy higher than **Ti-1S**. The Ti-C distances in **Ti-1T** suggest one η^4-C_4H_6 ligand and one $\eta^{3,3}$-C_8H_{12} ligand, thereby leading to a 14-electron configuration for the titanium atom.

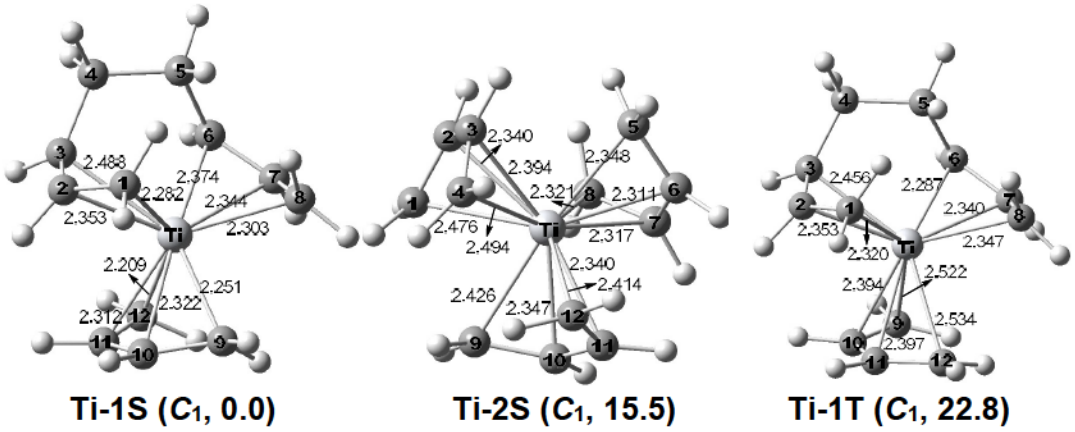

Figure 9. The low-energy optimized $(C_4H_6)_3Ti$ structures obtained by the B3LYP* method.

Table 7. Relative energies (ΔE in kcal/mol), relative energies with zero-point energy correction (ΔE_{ZPE} in kcal/mol), relative enthalpies (ΔH in kcal/mol), and spin expectation values $\langle S^2\rangle$ for the $(C_4H_6)_3Ti$ structures. None of the structures has any imaginary vibrational frequencies.

	Ti-1S (C_1)	Ti-2S (C_1)	Ti-1T (C_1)
ΔE	0.0	15.5	22.8
ΔE_{ZPE}	0.0	-0.9	3.8
ΔH(298K)	0.0	-0.1	4.1
$\langle S^2\rangle$	0.00	0.00	2.01

3.2 Dissociation Energies.

In order to investigate the stability of the $M(C_4H_6)_3$ complexes with respect to the dissociation of a C_4H_6 molecule, we have studied the following processes based on the

lowest energy structures and using results for the $M(C_4H_6)_2$ species are taken from previous research[7]:

$$M(C_4H_6)_3 \rightarrow M(C_4H_6)_2 + C_4H_6 \ (M = Ti, V, Cr, Mn, Fe, Co, Ni).$$

Table 8 lists the dissociation energies for the $M(C_4H_6)_3$ systems (M = Ti, V, Cr, Mn, Fe, Co, Ni). The dissociation energies for these $M(C_4H_6)_3$ systems range from 17 to 27 kcal/mol, with the smallest one (17 kcal/mol) for $Mn(C_4H_6)_3$. Thus, all the complexes in the present study are viable toward the removal of a C_4H_6 ligand. Since all of the lowest-energy $M(C_4H_6)_3$ isomers have coupled C_8H_{12} or $C_{12}H_{18}$ ligands, it seems that the significant dissociation energies may be attributed partially to the coupling of the C_4H_6 ligands.

Table 8. The classical dissociation energies (kcal/mol) for the successive removal of one butadiene group (C_4H_6) from $M(C_4H_6)_3$ (M = Ti, V, Cr, Mn, Fe, Co, Ni).

	B3LYP*
$Ti(C_4H_6)_3 \rightarrow Ti(C_4H_6)_2 + C_4H_6$	27.2
$V(C_4H_6)_3 \rightarrow V(C_4H_6)_2 + C_4H_6$	22.5
$Cr(C_4H_6)_3 \rightarrow Cr(C_4H_6)_2 + C_4H_6$	19.9
$Mn(C_4H_6)_3 \rightarrow Mn(C_4H_6)_2 + C_4H_6$	16.9
$Fe(C_4H_6)_3 \rightarrow Fe(C_4H_6)_2 + C_4H_6$	21.9
$Co(C_4H_6)_3 \rightarrow Co(C_4H_6)_2 + C_4H_6$	18.5
$Ni(C_4H_6)_3 \rightarrow Ni(C_4H_6)_2 + C_4H_6$	26.7

5. Discussion

The lowest energy $(C_4H_6)_3M$ (M = Ni, Co, Fe, Mn, Cr, V, Ti) structures for all first row transition metals contain an open chain $C_{12}H_{18}$ ligand formed by coupling the three C_4H_6 units. This ligand can be considered formally as a dianion so the central metal atoms in the $(C_{12}H_{18})M$ derivatives are in the formal +2 oxidation state. The $C_{12}H_{18}$ ligand in the lowest energy $(C_{12}H_{18})M$ structures can coordinate to the central metal atom either as hexahapto or octahapto ligands (Figure 10). Octahapto coordination of the open chain $C_{12}H_{18}$ ligand derived from three butadiene units without any hydrogen shifts involves all eight of the sp^2 carbon atoms, whereas there are two fundamentally different types of hexahapto $C_{12}H_{18}$ ligands, each leaving an uncomplexed C=C double bond in a different location. Octahapto $\eta^{3,2,3}$-$C_{12}H_{18}$ coordination and hexahapto $\eta^{3,3}$-$C_{12}H_{18}$ coordination both involve trihaptoallylic units at each end of the C_{12} chain.

Experimental work on first row transition metal $(C_4H_6)_3M$ complexes has restricted to the nickel system in view of its intermediacy in the nickel-catalyzed trimerization of butadiene to 1,5,9-cyclododecatriene. The rather unstable $C_{12}H_{18}Ni$ species isolated from nickel(0)/butadiene systems was shown by its hydrogenation to n-dodecane to contain a straight chain $C_{12}H_{18}$ ligand.[17] However, this species so far apparently has proven to be too labile for a definitive structure determination by X-ray crystallography. However, the cation $[\eta^{3,2,2}\text{-}C_{12}H_{19}Ni]^+$, formed by protonating $C_{12}H_{18}Ni$ with a strong acid has been characterized by X-ray diffraction.[18] An octahapto $\eta^{3,2,3}\text{-}C_{12}H_{18}Ni$ structure with the favored 18-electron configuration was originally suggested for the neutral unprotonated species.[8] However, our theoretical studies suggest a hexahapto structure $\eta^{3,3}\text{-}C_{12}H_{18}Ni$, corresponding to the lowest energy isomer **Ni-1S** with only a 16-electron nickel configuration (Figure 3). The local environment of the nickel atom in **Ni-1S** is similar to the stable bis(η^3-allyl)nickel, $(\eta^3\text{-}C_3H_5)_2Ni$, likewise a 16-electron complex.[42,43] The only other $C_{12}H_{18}Ni$ structures energetically within 25 kcal/mol of **Ni-1S** are three stereoisomers of hexahapto $\eta^{3,2,1}\text{-}C_{12}H_{18}Ni$, namely **Ni-2S**, **Ni-3S**, and **Ni-4S**. No octahapto $\eta^{3,2,3}\text{-}C_{12}H_{18}Ni$ structures are found at accessible energies.

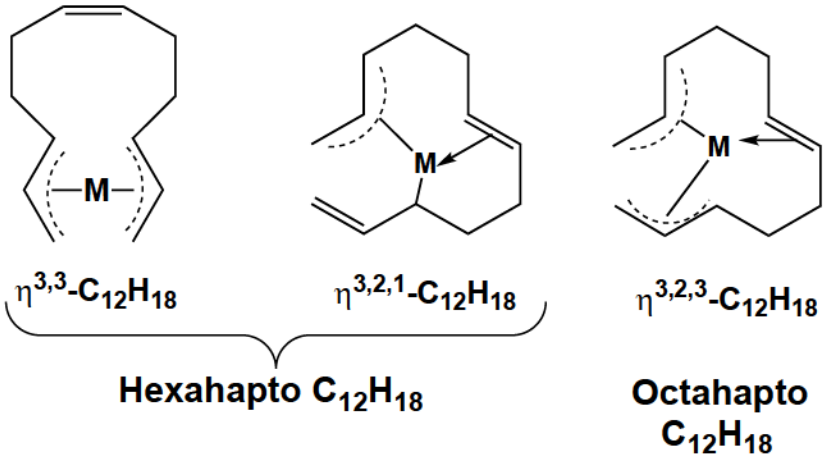

Figure 10. Schematic representation of the three fundamental modes of bonding of the $C_{12}H_{18}$ ligand in the lowest energy $C_{12}H_{18}M$ structures.

The $(C_4H_6)_3Co$ system is very similar to the $(C_4H_6)_3Ni$ system with the only structures within 20 kcal/mol of the lowest energy being the hexahapto $\eta^{3,3}\text{-}C_{12}H_{18}Co$ derivative **Co-1D** and the hexahapto $\eta^{3,2,1}\text{-}C_{12}H_{18}Co$ derivative **Co-2D**. However, for the $(C_4H_6)_3Fe$ system the lowest energy structures are the triplet $C_{12}H_{18}Fe$ structures **Fe-1T** and **Fe-2T** within ~1 kcal/mole in energy. Structure **Fe-2T** has a hexahapto

$\eta^{3,3}$-$C_{12}H_{18}$ ligand similar to **Ni-1S** and **Co-1D**, whereas **Fe-1T** has an octahapto $\eta^{3,2,3}$-$C_{12}H_{18}$ ligand.

The two lowest energy $(C_4H_6)_3Mn$ structures **Mn-1H** and **Mn-2H** have the same linear $C_{12}H_{18}$ ligands as found in the lowest energy $(C_4H_6)_3M$ structures of the later first row transition metals iron, cobalt, and nickel. However, these two structures are sextet spin state structures corresponding to the half-filled d shell of d^5 Mn(II). All other $(C_4H_6)_3Mn$ structures lie at least 20 kcal/mol in energy above these two structures. The ligands in **Mn-1H** and **Mn-2H** may be regarded as tetrahapto $\eta^{1,2,1}$-$C_{12}H_{18}$ bonding to the central manganese atom through only the carbon atoms at each end of the chain and the central C=C double bond. This mode of bonding leaves four uncomplexed C=C double bonds in the $C_{12}H_{18}$ chain.

A singlet (η^4- $C_4H_6)_3Cr$ structure with three tetrahapto butadiene ligands would be analogous to the very stable molybdenum and tungsten compounds[8,9] $(\eta^4$-$C_4H_6)_3M$ (M = Mo, W) and would have the favored 18-electron chromium configuration. Such a structure is found as **Cr-2S** (Figure 7 and Table 5) but this structure lies ~40 kcal/mol in energy above the lowest energy $(C_4H_6)_3Cr$ structure, namely **Cr-1P**, and is thus likely not be chemically significant. The lowest energy $(C_4H_6)_3Cr$ structures, namely the quintet structures **Cr-1P** and **Cr-2P**, have an open chain hexahapto $\eta^{3,3}$-$C_{12}H_{18}$ ligand, and are similar to the lowest energy $(C_4H_6)_3Ni$ structure **Ni-1S** (Figure 3) except for the spin state arising from the chromium atom having only a 14-electron configuration. The only other low-energy $(C_4H_6)_3Cr$ structure is the triplet $(\eta^{3,3}$-$C_8H_{12})(\eta^4$-$C_4H_6)Cr$ (**Cr-1T**) in which two of the three butadiene units have coupled to form a linear C_8H_{12} ligand.

The lowest energy $(C_4H_6)_3V$ structure **V-1Q** has an octahapto linear $C_{12}H_{18}$ ligand. A similar doublet $(\eta^{3,2,3}$-$C_{12}H_{18})V$ structure **V-1D** lies only ~4 kcal/mol in energy above **V-1Q**. The $(\eta^4$-$C_4H_6)_3V$ structure **V-2D** with three separate tetrahapto butadiene ligands and a 17-electron vanadium configuration is more energetically competitive than its chromium analogue $(\eta^4$-$C_4H_6)_3Cr$ (**Cr-2S**), since it lies only ~10 kcal/mol above the lowest energy isomer **V-1Q**.

Titanium is the only metal investigated here for which a structure with an open chain $C_{12}H_{18}$ ligand is not the lowest energy structure. Instead the lowest energy $(C_4H_6)_3Ti$ structure **Ti-1S** is of the $(\eta^{3,3}$-$C_8H_{12})(C_4H_6)Ti$ in which two of the three butadiene moieties have coupled to form an open chain hexahapto $\eta^{3,3}$-C_8H_{12} ligand. A $(\eta^4$-$C_4H_6)_3Ti$ structure **Ti-2S** with three separate tetrahaptobutadiene ligands and a 16-electron titanium configuration similar to stable sandwich compounds such as $(\eta^6$-$C_6H_6)_2Ti$ and $(\eta^5$-$C_5H_5)(\eta^7$-$C_7H_7)Ti$ lies ~15 kcal/mol above **Ti-1S**.

6. Conclusion

Our theoretical study suggests hexahapto $\eta^{3,3}$ rather than octahapto $\eta^{3,2,3}$ coordination for the open chain $C_{12}H_{18}$ ligand found in the unstable $C_{12}H_{18}Ni$ intermediate isolated during the nickel-catalyzed trimerization of butadiene. The lowest energy $(C_4H_6)_3M$ structures of the other first row transition metals from vanadium to cobalt are found to have related structures with open chain $C_{12}H_{18}$ ligands having hapticities ranging from four to eight with hexahapto structures being most common. The nickel and cobalt $(C_{12}H_{18})_3M$ derivatives favor low-spin singlet and doublet spin states, respectively, whereas the manganese derivative $(C_{12}H_{18})Mn$ favors the high-spin sextet state corresponding to the half-filled d^5 shell of Mn(II). A $(C_4H_6)_3Cr$ structure with three separate tetrahapto butadiene ligands analogous to the very stable $(\eta^4\text{-}C_4H_6)_3M$ (M = Mo, W) with the favored 18-electron metal configuration is found to be a very high energy structure relative to isomers containing an open chain $C_{12}H_{18}$ ligand.

Conflicts of Interest. There are no conflicts of interest to declare.

Acknowledgments. This study is supported by the Funds for Sichuan Distinguished Scientists of China (Grant Nos. 2019JDJQ0050 and 2019JDJQ0051), and the fund of the Key Laboratory of Advanced Scientific Computation, Xihua University, China. Research at the University of Georgia was supported by the U. S. National Science Foundation (Grant CHE-1661604).

Supporting Information. Tables S1 to S47: Atomic coordinates of the optimized structures for the $(C_4H_6)_3M$ (M =Ti, V, Cr, Mn, Fe, Co, Ni) complexes; Tables S48 to S94: Harmonic vibrational frequencies (in cm^{-1}) and infrared intensities (in parentheses in km/mol) for the $(C_4H_6)_3M$ (M =Ti, V, Cr, Mn, Fe, Co, Ni) complexes; Tables S95 to S101: The distances (in Å) of M-C bonds for the $(C_4H_6)_3M$ (M = Ti, V, Cr, Mn, Fe, Co, Ni) complexes; Tables S102 to S108: Total energies (E in hartree), relative energies (ΔE in kcal/mol), and the spin expectation $\langle S^2 \rangle$ values for the $(C_4H_6)_3M$ (M =Ti, V, Cr, Mn, Fe, Co, Ni) complexes by all four methods; complete Gaussian09 reference (Reference 39). Table S109: The theoretical (B3LYP*) Ni-C and C-C distances (in Å) of the $Ni(C_{12}H_{19})^+$ cation. The experimental results of those in $[Ni(C_{12}H_{19})]^+X^-$ (X = BF_4, F_3CSO_3) are listed for comparison. Table S110: The Mulliken spin density on the metal center. It shows that the spin states are mainly metal-centered, and the contributions from the ligand-based spin density are less than ±1.0, except for the high-energy **Ni-1T**.

References

(1) Kealy, T. J.; Pauson, P. L. A New Type of Organo-Iron Compound. *Nature* **1951**, *168*, 1039-1040.

(2) Miller, S. A.; Tebboth, J. A.; Tremaine, J. F. Dicyclopentadienyliron. *J. Chem. Soc.* **1952**, *3*, 632–635.

(3) Reihlen, O.; Gruhl, A.; Hessling, G.; Pfrengle, O. Über Carbonyle und Nitrosyle. IV. *Liebigs. Ann. Chem.* **1930**, *482*, 161-182.

(4) Hallam, B. F.; Pauson, P. L. Metal Derivatives of Conjugated Dienes. Part I. Butadiene- and cyclohexadiene-iron Tricarbonyls. *J. Chem. Soc.* **1958**, 642-645.

(5) Mills, O. S.; Robinson, G. Studies of Some Carbon Compounds of the Transition Metals. IV. The Structure of Butadiene Iron Tricarbonyl. *Acta Cryst.* **1963**, *16*, 758-761.

(6) Cloke, F. G. N.; Gardiner, M. G.; Raston C. L.; Simpson, S. J. Bis{1,4-bis(trimethylsilyl) buta-1,3-diene}cobalt: Synthesis and Molecular Structure *J. Organomet. Chem.,* **1996**, 507, 245-248.

(7) Fan, Q. C.; Li, H. D.; Feng, H.; Sun, W. G.; Xie, Y. M.; King, R. B.; Schaefer H. F. Butadiene as a Ligand in Open Sandwich Compounds, *Phys. Chem. Chem. Phys.* **2018**, *20*, 5683-5691.

(8) Skell, P. S.; VanDam, E. M.; Simon, M. P. Reactions of Tungsten and Molybdenum Atoms with 1,3-Butadiene. Tris (Butadiene) Tungsten and Molybdenum. *J. Am. Chem. Soc.* **1974**, *96*, 626-627.

(9) Gausing, W.; Wilke, G. Reduktive Synthese und Reaktivität von Tris (butadien) molybdän und-wolfram. *Angew. Chem.* 1981, *93*, 201-202.

(10) Wilke, G.; Bogdanovic, B.; Borner, P.; Breil, H.; Hardt, P.; Heimbach, P.; Herrmann, G.; Kaminsky, H. -J.; Keim, W.; Kröner, M.; Müller, H., Müller, E. W.; Oberkirch, W.; Schneider, J.; Stedefeder, J.; Tanaka, K.; Weyer, K.; Wilke, G. Cyclooligomerization of Butadiene and Transition Metal π-Complexes. *Angew. Chem. Int. Ed.* **1963**, *2*, 105-164.

(11) Wilke, G. Contributions to Organo-Nickel Chemistry. *Angew. Chem. Int. Ed.* **1988**, *27*, 185-206.

(12) Wilke, G. Eckerle, A. In *Applied Homogeneous Catalysis with Organometallic Complexes;* Cornils, B.; Herrmann, W. A., Eds.; VCH, Weinheim, Germany, 1996; pp. 358–373.

(13) Wilke, G. Organo Transition Metal Compounds as Intermediates in Homogeneous Catalytic Reactions. *Pure Appl. Chem.* **1978**, *50*, 677-690.

(14) Wilke, G. Contributions to Homogeneous Catalysis 1955–1980. *J. Organomet. Chem.* **1980**, *200*, 349-364.

(15) Skell, P. S.; Havel, J. J.; Williams-Smith, D. L.; McGlinchey, M. J. Reactions of Nickel Atoms with Unsaturated Hydrocarbons. *J. Chem. Soc. Chem. Commun.* **1972**, 1098-1099.

(16) Jolly, P. W.; Mynott, R.; Salz, R. Bis(η^4-2,3-dimethyl-1,3-butadiene) Nickel. *J. Organomet. Chem.* **1980**, *184*, C49-C52.

(17) Wilke, G.; Kröner, M.; Bogdanović, B. Ein Zwischenprodukt der Synthese von Cyclododecatrien aus Butadien. *Angew. Chem.* **1961**, *73*, 755-756.

(18) Taube, R.; Langlotz, J.; Sieler, J.; Gelbrich, T.; Tittes, K. Komplexkatalyse LVI: Zur Kation-Anion-Wechselwirkung in den C_{12}-Allylnickel(II)-Komplexen $[Ni(\eta^3,\eta^2,\eta^2\text{-}C_{12}H_{19})]X$ als Steuergröße für die Katalyse der stereospezifischen Butadienpolymerisation. Synthese des Tetrakis(pentafluorphenyl)borats (X = $B(C_6F_5)_4$) und Charakterisierung des Tetrafluoroborats sowie des Trifluormethansulfonats (X = BF_4, CF_3SO_3) durch Röntgenkristallstrukturanalyse und Leitfähigkeitsmessungen. *J. Organomet. Chem.* **2000**, *597*, 92–104.

(19) Brauer, D. J.; Krüger. C. The Three-dimensional Structure of Trans. Trans, Trans-1,5,9-cyclododecatrienenickel. *J. Organomet. Chem.* **1972**, *44*, 397-402.

(20) Tobisch, S. Ni^0-Catalyzed Cyclotrimerization of 1,3-Butadiene: A Comprehensive Density Functional Investigation on the Origin of the Selectivity. *Chem. Eur. J.* **2003**, *9*, 1217-1232.

(21) Ziegler, T.; Autschbach, J. Theoretical Methods of Potential Use for Studies of Inorganic Reaction Mechanisms. *Chem. Rev.* **2005,** *105*, 2695-2722.

(22) Bühl, M.; Kabrede, H. Geometries of Transition-Metal Complexes from Density-Functional Theory. *J. Chem. Theory Comput.* **2006**, *2,* 1282-1290.

(23) Brynda, M.; Gagliardi, L.; Widmark, P. O.; Power, P. P.; Roos, B. O. A Quantum Chemical Study of the Quintuple Bond between Two Chromium Centers in [PhCrCrPh]: trans-Bent versus Linear Geometry. *Angew. Chem. Int. Ed.* **2006**, *45*, 3804-3807.

(24) Sieffert, N.; Bühl, M. Hydrogen Generation from Alcohols Catalyzed by Ruthenium-Triphenylphosphine Complexes: Multiple Reaction Pathways. *J. Am. Chem. Soc.* **2010**, *132*, 8056-8070.

(25) Schyman, P.; Lai, W.; Chen, H.; Wang, Y.; Shaik, S. The Directive of the Protein: How Does Cytochrome P450 Select the Mechanism of Dopamine Formation? *J. Am. Chem. Soc.* **2011,** *133*, 7977-7984.

(26) Adams, R. D.; Pearl Jr., W. C.; Wong, Y. O.; Zhang, Q.; Hall, M. B.; Walensky, J. R. Tetrarhena-heterocycle from the Palladium-Catalyzed Dimerization of $Re_2(CO)_8(\mu\text{-}SbPh_2)(\mu\text{-}H)$ Exhibits an Unusual Host-Guest Behavior. *J. Am. Chem. Soc*. **2011**, *133*, 12994-12997.

(27) Lonsdale, R.; Oláh, J.; Mulholland, A. J.; Harvey, J. N. Does Compound I Vary Significantly between Isoforms of Cytochrome P450? *J. Am. Chem. Soc.* 2011, *133*, 15464-15474.

(28) Papadopoulou, A.; Becker, E. D.; Lupkowski, M.; van Swol, F. Molecular Dynamics and Monte Carlo Simulations in the Grand Canonical Ensemble: Local versus global control. *J. Chem. Phys.* **1993**, *98*, 4897-4908.

(29) Lee, C.; Yang, W.; Parr, R. G. Development of the Colle-Salvetti Correlation-Energy Formula into a Functional of the Electron Density. *Phys. Rev. B* 1988, *37*, 785-789.

(30) Becke, A. D. Density-functional Exchange-energy Approximation with Correct Asymptotic Behavior. *Phys. Rev. A* **1988**, *38*, 3098-3100.

(31) Perdew, J. P. Density-functional Approximation for the Correlation Energy of the Inhomogeneous Electron Gas. *Phys. Rev. B* **1986**, *33*, 8822-8824.

(32) Reiher, M.; Salomon, O.; Hess, B. A. Reparameterization of Hybrid Functionals Based on Energy Differences of States of Different Multiplicity. *Theor. Chem. Acc.* **2001**, *107*, 48-55.

(33) Salomon, O.; Reiher, M.; Hess, B. A. Assertion and Validation of the Performance of the B3LYP* Functional for the First Transition Metal Row and the G2 Test Set. *J. Chem. Phys.* **2002**, *117*, 4729-4237.

(34) Zhao Y.; Truhlar. D. G. The M06 Suite of Density Functionals for Main Group Thermochemistry, Thermochemical Kinetics, Noncovalent Interactions, Excited States, and Transition Elements: Two New Functionals and Systematic Testing of Four M06-Class Functionals and 12 Other Functionals. *Theor. Chem. Acc.* **2008**, *120*, 215-241.

(35) Dunning Jr., T. H. Gaussian Basis Functions for Use in Molecular Calculations. I. Contraction of (9s5p) Atomic Basis Sets for the First-Row Atoms. *J. Chem. Phys.* **1970**, *53*, 2823-2833.

(36) Huzinaga, S. Gaussian-Type Functions for Polyatomic Systems. I. *J. Chem. Phys.* **1965**, *42*, 1293-1302.

(37) Wachters, A. J. H. Gaussian Basis Set for Molecular Wavefunctions Containing Third-Row Atoms. *J. Chem. Phys.* **1970**, *52*, 1033-1036.

(38) Hood, D. M.; Pitzer, R. M.; Schaefer, H. F. Electronic Structure of Homoleptic Transition Metal Hydrides: TiH_4, VH_4, CrH_4, MnH_4, FeH_4, CoH_4, and NiH_4. *J. Chem. Phys*. **1979**, *71*, 705-712.

(39) Frisch, M. J.; Trucks, G. W.; Schlegel, H. B.; Scuseria, G. E.; Robb, M. A.; Cheeseman, J. R.; Scalmani, G.; Barone, V.; Mennucci, B.; Petersson, G. A., *et al. Gaussian 09,* Revision B.01; Gaussian, Inc., Wallingford CT, 2010.

(40) Ang, L. S.; Sulaiman, S.; M. I. Mohamed-Ibrahim, *Sains Malaysiana*, Effects of Spin Contamination on the Stability and Spin Density of Wavefunction of Graphene: Comparison between First Principle and Density Functional Methods, **2012**, 41, 445-452.

(41) Zeinstra, J. D.; De Boer, J. L. Structure of Cyclopentadienylcycloheptatrienyl-titanium, *J. Organomet. Chem.* **1973**, *54*, 207-211.

(42) Wilke, G.; Bogdanović, B.; Hardt, P.; Heimbach, P.; Keim, W.; Kröner, M.; Oberkirch, W.; Tanaka, K.; Steinrücke, E.; Walter, D.; Zimmermann. H. Allyl-Transition Metal Systems, *Angew. Chem. Int. Ed.* **1966**, *5*, 151-164.

(43) Bönnemann, H.; Bogdanović, B.; Wilke, G. cis-and trans-Bis-(π-allyl) nickel Systems, *Angew. Chem. Int. Ed.* **1967**, *6*, 804-804.

TOC Graphic

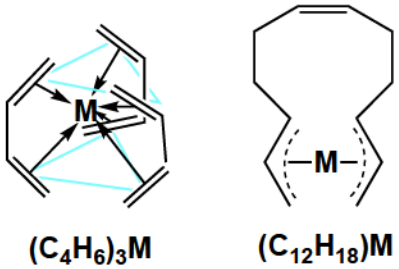

$(C_4H_6)_3M$ $(C_{12}H_{18})M$